

Supplemental Material

Detailed Methods

Generation of *Chop*^{fl/fl} (*Ddit3*^{fl/fl}) mice in the C57BL/6J background

Using a bacteria artificial chromosome (BAC), exon 3 of the *Ddit3* gene was flanked with a *LoxP* (L83) site and a Frt-Neo-Frt-Loxp (FNFL) cassette. The following three elements were then ligated into a gene-targeting vector carrying the DTA (diphtheria toxin alpha chain) negative-selection marker: a 2-kb short homology arm (5' to L83), the above *LoxP*-exon 3-FNFL sequence, and a 5-kb long homology arm (end of FNFL to 3'). The FNFL cassette conferred G418 resistance during gene targeting in CSL2J2 ES cells (derived from B6(Cg)-*Tyr*^{cr-2J}/J mice; JAX Mice Stock number: 000058), and the DTA cassette provided an autonomous negative selection strategy to reduce random integration events during gene targeting. Several targeted ES cells were identified and injected into C57BL/6J blastocysts to generate chimeric mice. Male chimeras were bred to ACTB (Flpe/Flpe) females in the C57BL/6J background to transmit through germ line the floxed *Ddit3* allele, *i.e.*, L83/FL146 allele with neo cassette removed by Fpe recombinase (**Online Figure I**). The ES cells and mice carrying the floxed *Ddit3* allele were genotyped with the primers designated in **Online Table I**. Founder mice heterozygous for the Chop floxed allele were further cross-bred to generate littermates homozygous for Chop floxed gene (*Chop*^{fl/fl} mice).

Verification of successful *Chop* gene deletion *in vivo*

Chop^{fl/fl} mice were challenged with adenovirus encoding the *Cre* recombinase through tail vein injection, followed by treatment with Tm 2 mg/kg for 8 h. Protein and DNA were prepared from liver and/or spleen. Deletion of the exon 3 of *Chop* gene was verified by gel electrophoresis and sanger sequencing of the PCR product from liver genomic DNA using primers (**Online Table I**) amplifying the region flanked by the two *LoxP* sites; deletion of CHOP protein in liver was verified by western blotting.

Generation of *Chop*^{fl/fl} *Apoe*^{-/-} and *Chop*^{fl/fl} *SM22α-CreK1*⁺ *Apoe*^{-/-} mice and diets

To generate *Chop*^{fl/fl} *Apoe*^{-/-} mice, the *Chop* exon 3-floxed (*Chop*^{fl/fl}) mice were bred with *Apoe*^{-/-} mice (in C57BL/6J background; JAX Mice Stock number: 002052) to introduce an atherosclerosis-prone genetic background. To generate SMC-specific *Chop*-deficient

mice, *Chop^{fl/fl}Apoe^{-/-}* mice were further bred with a SM22 α -CreKI transgenic mice in C57BL/6J background.¹ Distinct from endogenous SM22 α expression, SM22 α -CreKI mice express Cre recombinase in adult but not embryonic SMCs.¹ Starting at 6 wks of age, male *Chop^{fl/fl}Apoe^{-/-}* and *Chop^{fl/fl}SM22 α -CreK1⁺Apoe^{-/-}* mice were fed a 21.2% fat, 0.2% cholesterol Western-type diet (Harlan Teklad, Madison, WI; catalog #TD88137) for 12 wks.

Blood glucose and plasma lipid analysis

At the end of the study, the mice were fasted overnight. A drop of blood was collected from mouse tail, and blood glucose was measured using a glucose meter (One Touch Ultra, Lifescan). Mice were then weighed, anesthetized using isoflurane, and euthanized. Blood was collected from the left ventricle for lipid analysis. Total plasma triglyceride and cholesterol and HDL-cholesterol were measured with a commercially available kit from Wako. Plasma lipoprotein profiles were determined by fast performance liquid chromatography (FPLC) gel filtration on a Superose 6 column at a flow rate of 0.2 ml per minute. Eluted fractions were assayed for cholesterol. All mouse protocols were approved by the Columbia University Institutional Animal Care and Use Committee.

Atherosclerotic lesion analysis

Mouse hearts were perfused *in-situ* with saline and removed. The aortic root or aortic arch was placed in OCT medium and immediately frozen. Using a cryomicrotome, sections were cut serially at 8- μ m intervals starting from the aortic sinus and then mounted on slides. For lesion area analysis, the sections were stained with eosin and hematoxylin, and intimal lesion area was quantified by averaging measurements from 6 sections, 50 μ m apart, using a Nikon Labophot 2 microscope and Image Pro Plus image analysis software. To measure *en face* aortic lesion area, the thoracic aorta was dissected from the heart and surrounding tissues and the adventitial fat tissue was cleaned and incubated overnight in 10%-buffered formalin. The aorta was then splayed open longitudinally under a dissecting microscope and pinned to silicone-coated plates, and Oil red O staining was performed. Images were acquired, and Oil red O-positive area was analyzed by applying a color threshold in Adobe Photoshop.

Measurement of Blood Pressure

Blood pressure was measured using a noninvasive computerized tail–cuff system (Kent Scientific Corporation, CT, USA). After the mice were placed in a plastic holder, the occlusion and sensor cuff were positioned on the base of the tail. After the mice were given time to adapt to the system, blood pressure was measured for at least three consecutive times in each mouse.

Immunochemistry and microscopy

Immunochemistry on frozen aortic root sections were performed as described previously.² Briefly, frozen sections were fixed in ice-cold acetone for 5 min and then blocked with normal serum. Sections were labeled with unconjugated primary antibodies against smooth muscle α -actin (Sigma-Aldrich), CD11c, F4/80 (BD biosciences), Ki67 (Cell signaling), KLF4 (Millipore, or R & D Systems), ATF4 (Santa Cruz or Cell signaling), or activated caspase 3 (Cell Signaling) overnight, followed by fluorophore-conjugated secondary antibody for 1 h. The stained sections were mounted with DAPI-containing Vectorshield mounting medium (Vector) and then viewed using an Olympus IX 70 fluorescence microscope. The images were analyzed using ImageJ. Confocal microscopy was conducted using a Nikon Ti Eclipse inverted microscope. The Z series was obtained by imaging serial confocal planes (3 planes at 1.2- μ m intervals) at 1024 x 1024 pixel resolution with a Nikon 20x objective. Projections of the Z-stacks were generated, and co-localization analysis was performed by NIS software (Nikon, NY, USA).

Masson's trichrome staining

Paraffin-embedded aortic root sections were de-paraffinized and then stained with a Masson's trichrome stain kit from Sigma-Aldrich. Collagen, which was stained with Aniline blue in the kit, was quantified using ImageJ.

Isolation and culture of mouse aortic vascular smooth muscle cells (VSMCs)

VSMCs were isolated from mouse thoracic aorta by an enzymatic digestion method.³ Cells were cultured in DMEM/F12 medium (GIBCO) supplemented with 20% FBS, penicillin/streptomycin 100U/ml before passage 6. After passage 6, cells were cultured with 10% FBS medium and used between passage 6 and 10. For serum starvation, cells were cultured with DMEM/F12 supplemented with L-glutamine 1.6 mM (Gibco), L-

ascorbic acid 0.2 mM (Sigma-Aldrich), transferrin 5 µg/ml (Sigma-Aldrich), insulin 2.8 µg/ml (Gibco), penicillin/streptomycin 100 U/ml (Gibco), and Na-selenate 6.25 ng/ml (Sigma-Aldrich) for 2-3 days.

Isolation and culture of mouse lung endothelial cells (ECs)

ECs were isolated from mouse lung after digestion with collagenase as described previously.⁴ Briefly, after two passages of total lung cell culture, ECs were isolated using magnetic Dynabeads (Invitrogen) conjugated with ICAM-2 antibody (BD Pharmingen). Cells were cultured in DMEM low glucose medium (GIBCO) supplemented with 10% horse serum, penicillin/streptomycin 100U/ml, L-glutamine 1.6 mM, ECGS 50 µg/ml (Biomedical Technologies), and heparin 100 µg/ml (Sigma-Aldrich). The first two passages of ECs were used in experiments.

Isolation and culture of mouse bone marrow-derived macrophages

Bone marrow-derived macrophages were separated as described previously.⁵ To prepare bone marrow-derived macrophages, both ends of femurs were removed, and the marrow was flushed with RPMI medium. The flushed cells were placed through a strainer to remove debris and then pelleted by centrifugation. The cells were re-suspended in DMEM containing 20% L-cell-conditioned medium, cultured for 4-5 days, and then used for the experiments.

***In vitro* proliferation assay**

VSMC proliferation was measured as previously described.⁶ Briefly, serum-starved VSMCs were incubated with cell culture medium with 10% FBS at 37°C in a CO₂ incubator. After culture for 0-4 days after serum starvation, cells were collected by trypsin digestion and counted with a hemocytometer.

Immunoblotting

Cells were lysed in a buffer containing 2% SDS, 62.5 mM Tris-HCl (pH 6.8), 10% glycerol, 50 mM DTT, and 0.01% bromphenol blue and boiled at 100°C for 5 min. Lysate protein was separated on 4-20% gradient SDS-PAGE gel (Invitrogen) and electrotransferred to 0.4-µm PVDF membrane. The membranes were blocked for 1 h at room temperature in Tris-buffered saline and 0.1% Tween 20 (TBST) containing 5% (wt/vol) nonfat milk. The membranes were then incubated with primary antibody against

Chop (Santa Cruz), β -actin (Santa Cruz), KLF4 (Millipore), p-eIF2 α and eIF2 α (Cell Signaling), ATF4 (Santa Cruz), or GAPDH (Cell signaling) in TBST containing 5% nonfat milk at 4°C overnight, and the protein bands were detected with horse radish peroxidase-conjugated secondary antibodies (Cell signaling) and Supersignal West Pico enhanced chemiluminescence solution (Pierce).

Quantitative RT-qPCR

Total RNA was extracted from HCs using the RNeasy kit (Qiagen). cDNA was synthesized from 2 μ g total RNA using oligo (dT) and Superscript II (Invitrogen). qPCR was performed in an 7500 Real time PCR system (Applied Biosystems) using SYBR green chemistry. QuantiTect primers for *Klf4*, *Gadd34*, *Hprt*, and *Actb* were used (Qiagen).

siRNA-mediated gene silencing

siRNA sequences against murine *Klf4*, *Atf4* and scrambled RNA, were purchased from Qiagen; the target sequence of *Klf4* siRNA was CCGGTTTATATTGAATCCAAA , the target sequence of *Atf4* siRNA was GACUGAGAAAUUGGAUAAGAAGCTG. The scrambled RNA and siRNA were transfected into SMCs using the basic nucleofector kit for primary SMCs and Amaxa nucleofector (Lonza) according to the manufacturer's instruction.

Chromatin immunoprecipitation (ChIP)

Atf4^{+/+} and *Atf4*^{-/-} MEFs were treated with 2 μ g/ml tunicamycin (Sigma-Aldrich) for 8 h, followed by cross-linking with 1% formaldehyde for 10 min and subsequent chromatin immunoprecipitation as described, using anti-ATF4 antibody (gift from Dr. Michael S. Kilberg, University of Florida College of Medicine).⁷ DNA immunoprecipitates were analyzed by RT-qPCR using the following primers: *Klf4* intron1 (5'- CTC AGC TAA CAC CAA GGT AAG A-3' and 5'- TGT CCC AGT GTC CCA ATT C-3'), p*Klf4* #1 (5'- AGT TCC AGC TCA CAA CTC ATC-3' and 5'- TAA CTC TTC TGG CCC TAC CT-3'), p*Klf4* #2 (5'- CAA CAG CCT TCT GGA GGA TAA A-3' and 5'- GGA TGA GTT GTG AGC TGG AA-3'), p*Klf4* #3 (5'- AGA TGA ATT GGA GAG CCA CTA TT-3' and 5'- AGA AGG CTG TTG GGA AAC TT-3'), and *Trb3* (5'- aac tca acg atc cac ctg cct ct-3' and 5'- aac ctg agc taa tct gct gct gac-3'). Data were plotted as the ratio to the value obtained with 1:20 dilution of input DNA.

Ubiquitin assay

For immunoprecipitation, VSMCs from one 100-mm dish were infected with adenovirus encoding *Klf4*. After 3 days, the cells were treated with MG132 for 6 h and then lysed in IP buffer (1.2 ml of 20 mM Tris-HCl pH 7.4, 100 mM NaCl, 10% glycerol, 1% NP-40, 12.5 mM N-ethylmaleimide). The lysate was mixed with 5 µg anti-KLF4 antibody and rotated at 4°C overnight, followed by adding 100 µl protein G beads and rotating for additional 2 hours at 4°C. The beads were washed three times by vortexing in IP buffer, followed by centrifugation for 5 s at 10 000 x *g*. The IP pellet was boiled in 2X SDS sample buffer and subjected to immunoblot analysis.

Statistical Analysis

Data are displayed as mean ± S.E.M., with the n number given in the individual figure legends. After the data were shown to fit a normal distribution, the unpaired t-test was used to assess the statistical significance of the differences in experiments with two groups, and two-way ANOVA was used for analyses in multi-group experiments.

References

1. Zhang J, Zhong W, Cui T, Yang M, Hu X, Xu K, Xie C, Xue C, Gibbons GH, Liu C, Li L and Chen YE. Generation of an adult smooth muscle cell-targeted Cre recombinase mouse model. *Arterioscler Thromb Vasc Biol.* 2006;26:e23-4.
2. Wang Y, Wang GZ, Rabinovitch PS and Tabas I. Macrophage mitochondrial oxidative stress promotes atherosclerosis and nuclear factor-kappaB-mediated inflammation in macrophages. *Circ Res.* 2014;114:421-33.
3. Geisterfer AA, Peach MJ and Owens GK. Angiotensin II induces hypertrophy, not hyperplasia, of cultured rat aortic smooth muscle cells. *Circ Res.* 1988;62:749-56.
4. Hartwell DW, Mayadas TN, Berger G, Frenette PS, Rayburn H, Hynes RO and Wagner DD. Role of P-selectin cytoplasmic domain in granular targeting in vivo and in early inflammatory responses. *J Cell Biol.* 1998;143:1129-41.
5. Liao X, Sluimer JC, Wang Y, Subramanian M, Brown K, Pattison JS, Robbins J, Martinez J and Tabas I. Macrophage autophagy plays a protective role in advanced atherosclerosis. *Cell Metab.* 2012;15:545-53.
6. Stouffer GA and Owens GK. TGF-beta promotes proliferation of cultured SMC via both PDGF-AA-dependent and PDGF-AA-independent mechanisms. *J Clin Invest.* 1994;93:2048-55.
7. Han J, Back SH, Hur J, Lin YH, Gildersleeve R, Shan J, Yuan CL, Krokowski D, Wang S, Hatzoglou M, Kilberg MS, Sartor MA and Kaufman RJ. ER-stress-induced transcriptional regulation increases protein synthesis leading to cell death. *Nat Cell Biol.* 2013;15:481-90.

Online Table I. Primers used for genotyping and verification of *Chop* floxed mice.

Primers	Sequences
Ddit3screen1F	GCTTTTTCCCCATTCATTCCTAACA
Ddit3screen1R	CCTCGAGGGACCTAATAACTTCGTA
Ddit3LNL5F	AAGTGCATCTTCATACACCACCACA
Ddit3LNL3R	TCCCAAGTGCTGGGACTAAAGGTAT
Ddit3FNFL5F	GAGGTGAGTGAGAATGCTGGTCCTA
Ddit3FNFL3R	TTCTTCCTTGCTCTTCCTCCTCTTC
PCR verification	Forward: CCTCTCAGTCAGCTGCGAAT Reverse: ACCATTTCCCTGCGATGCTA
Sanger sequencing	Forward: AGCCGATCATATTCAATAACCCTTA Reverse: ACCATTTCCCTGCGATGCTA

Online Figure Legends

Online Figure I. Generation of *Chop*^{fl/fl} mice and VSMC-targeted CHOP-deficient mice on the *Apoe*^{-/-} background. **A**, Scheme of *Chop* DNA and insertion of 2 *LoxP* sites flanking exon 3 and Southern blots confirming genotypes of positive ES cells and the indicated mice. **B**, Deletion of *Chop* gene in liver by ectopic expression of *Cre* recombinase (Ad-*Cre*) efficiently abolished CHOP protein expression in response to tunicamycin (Tm) administration (i.p., with mice sacrificed 8 h post injection), while PBS-sham injected *Chop*^{fl/fl} mice displayed CHOP protein induction at the predicted molecular weight of CHOP (~29 kDa). Lv, liver; Sp, spleen. **C**, A 1.2 kb PCR product corresponding to the *LoxP*-recombined genomic sequence was evident in the liver of adeno-*Cre* administered mouse, while the product was absent in the PBS sham-injected *Chop*^{fl/fl} mice. **D**, Sanger sequencing of the PCR product confirmed *LoxP* insertion sites at the predicted locations, with the left arm inserted in the second intron of the *Chop* gene and the right arm inserted in the third intron. The underlined nucleotides represent the intronic region endogenous to the *Chop* gene, along with the adjacent nucleotides of the inserted *LoxP* sites (non-essential sequences not shown). The sequencing result also confirmed intact exon 4 sequence of the *Chop* gene demonstrating precise excision of exon 3 upon *Cre* recombinase expression (data not shown).

Online Figure II. Generation of VSMC-targeted CHOP-deficient mice on the *Apoe*^{-/-} background. **A**, Breeding scheme for generating *Chop*^{fl/fl}*Apoe*^{-/-} and *Chop*^{fl/fl}*SM22 α -Cre*^{+/+}*Apoe*^{-/-} mice. **B**, Immunoblots of CHOP in aortic VSMCs, lung ECs, and bone marrow-derived macrophages (Mf) isolated from *Chop*^{fl/fl}*Apoe*^{-/-} and *Chop*^{fl/fl}*SM22 α -Cre*^{+/+}*Apoe*^{-/-} mice before and after 12 h tunicamycin (Tm) treatment. b-actin was used as loading control.

Online Figure III. Body weight and systemic metabolic factors are similar in *Chop*^{fl/fl}*Apoe*^{-/-} and *Chop*^{fl/fl}*SM22 α -Cre*^{+/+}*Apoe*^{-/-} mice. **A-E**, Body weight, fasting blood glucose, plasma triglyceride, plasma cholesterol, and HDL cholesterol of Western diet-fed male *Chop*^{fl/fl}*Apoe*^{-/-} and *Chop*^{fl/fl}*SM22 α -Cre*^{+/+}*Apoe*^{-/-} mice (n=14). **F**, Pooled plasma samples were subjected to fast performance liquid chromatography gel filtration, and the fractions were assayed for cholesterol concentration. **G-H**, Systolic and diastolic blood pressure in 12-wk WD-fed *Chop*^{fl/fl}*Apoe*^{-/-} and *Chop*^{fl/fl}*SM22 α -*

CreK1⁺Apoe^{-/-} mice (n=5). None of the differences between the two groups of mice was statistically significant.

Online Figure IV. CHOP deletion in VSMCs in *Apoe^{-/-}* mice reduces the content of F4/80⁺ macrophage, CD11c⁺ cells, and collagen in aortic root lesions.

Aortic root lesions of *Chop^{fl/fl}Apoe^{-/-}* and *Chop^{fl/fl}SM22 α -CreK1⁺Apoe^{-/-}* mice were immunostained for F4/80 or CD11c (A-B) or stained with Masson trichrome and analyzed for Aniline blue (collagen) staining (C). Total stained area and stained area per lesion area were quantified (n=8).

Online Figure V. CHOP deletion in VSMCs in *Apoe^{-/-}* mice reduces the content of a-actin⁺ cells in aortic arch lesions, but not non-atherosclerotic aorta, and decreases lesion size in both the aortic arch and descending aorta. A,

Representative images of aortic arch cross-sections in *Chop^{fl/fl}Apoe^{-/-}* and *Chop^{fl/fl}SM22 α -CreK1⁺Apoe^{-/-}* mice. B, Quantitative analyses of lesion area in the aortic arch (n=4). C, Quantitative analyses of a-actin⁺ cells in aortic arch lesions (n=4). D, Representative *en face* images and quantification of Oil Red O-stained descending aorta from *Chop^{fl/fl}Apoe^{-/-}* and *Chop^{fl/fl}SM22 α -CreK1⁺Apoe^{-/-}* mice (n=3). E, Quantification of α -actin⁺ cells in the aortic wall of non-atherosclerotic chow-fed *Chop^{fl/fl}* and *Chop^{fl/fl}SM22 α -CreK1⁺* mice (n=6; n.s., non-significant).

Online Figure VI. Apoptosis of a-actin⁺ cells is similar in aortic root lesions of *Chop^{fl/fl}Apoe^{-/-}* and *Chop^{fl/fl}SM22 α -CreK1⁺Apoe^{-/-}* mice. A,

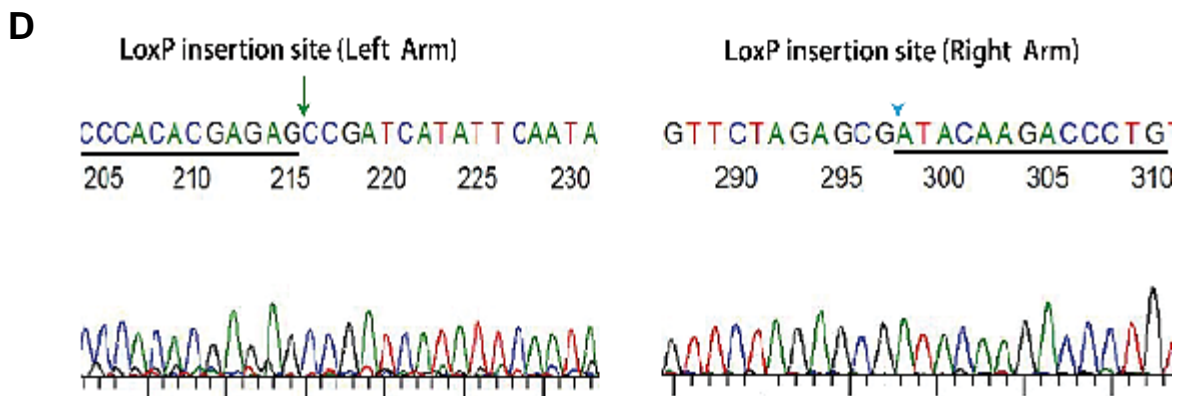
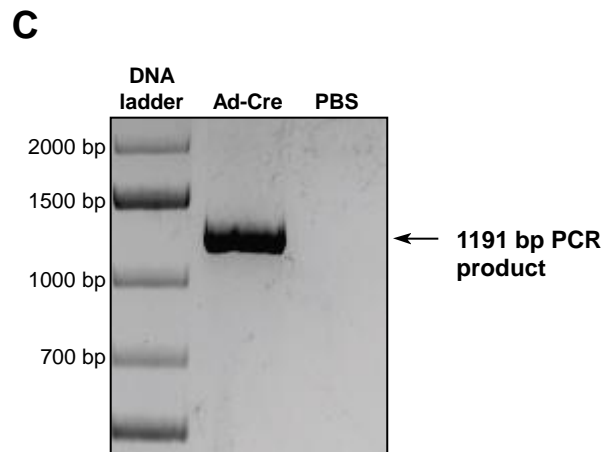
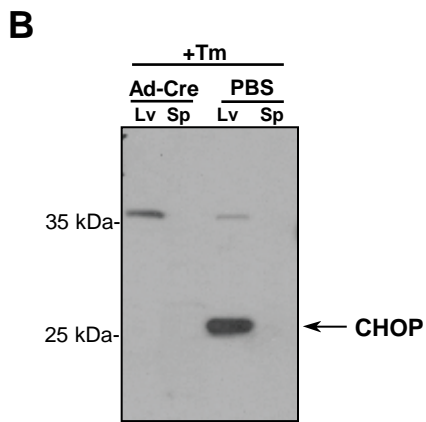
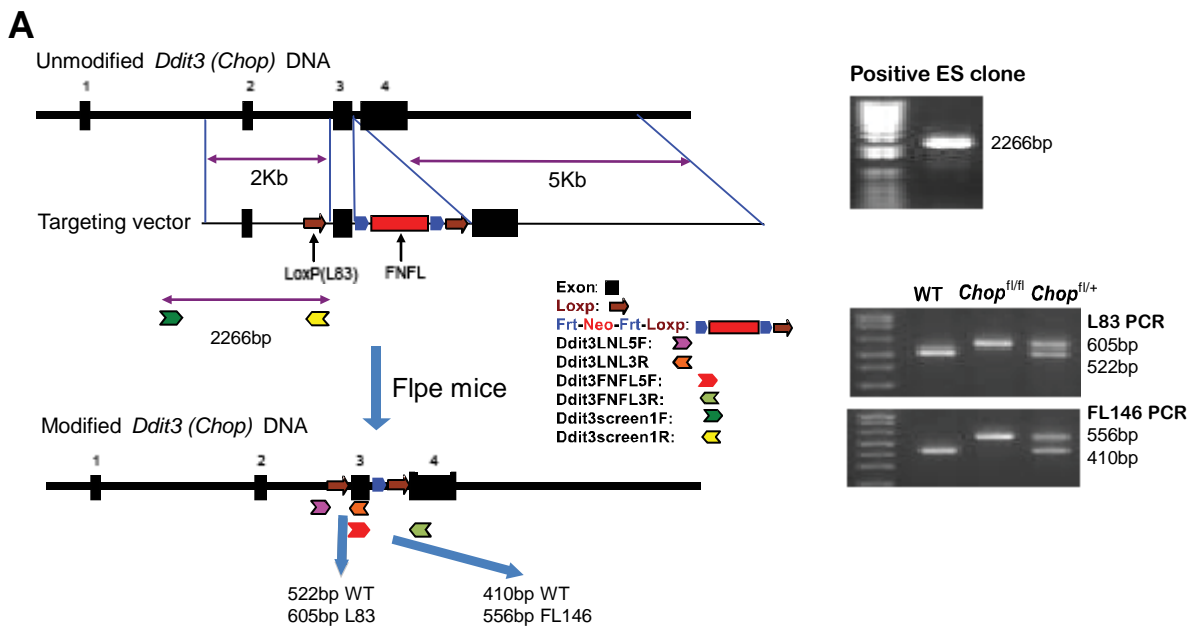
Representative images of DAPI (blue), α -actin (green), and active-caspase 3 (red) staining in *Chop^{fl/fl}SM22 α -CreK1⁺Apoe^{-/-}* lesions. Arrow, active caspase 3 staining that coincides with an α -actin⁺ cell. Bar, 20 μ m. B, Quantification of α -actin/active caspase 3 double-positive lesional cells. C, Correlation analysis of α -actin/active Casp3 double-positive cells with total lesional VSMCs. For B-C, n=8 per cohort.

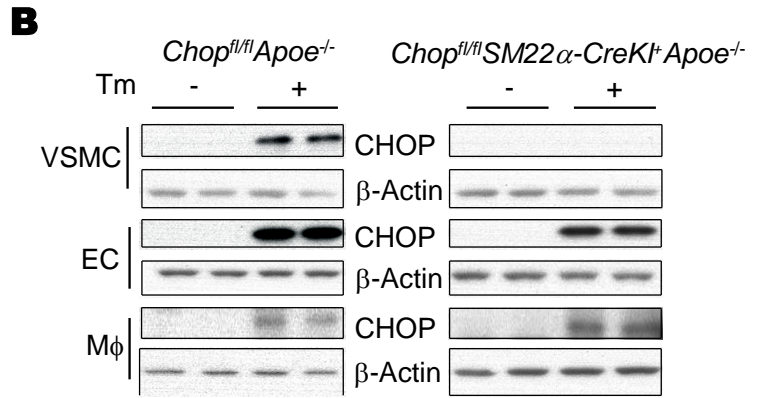
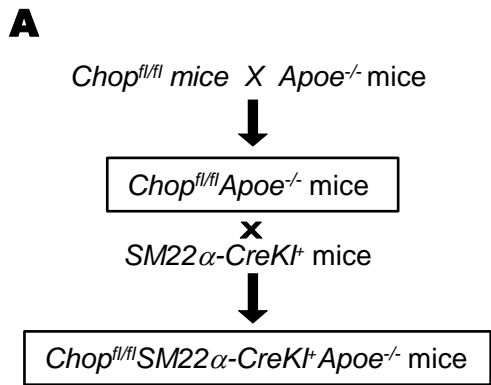
Online Figure VII. VSMC-CHOP deficiency is associated with a higher percentage of total lesional cells that co-stain for nuclear ATF4 and KLF4 and of a-actin⁺ lesional cells that stain for nuclear ATF4. A,

Representative Z series projection images of KLF4 (Green), ATF4 (Red), and DAPI (blue) staining in *Chop^{fl/fl}SM22 α -CreK1⁺Apoe^{-/-}* lesions and percentage of KLF4/ATF4/DAPI triple-stained nuclei in 9

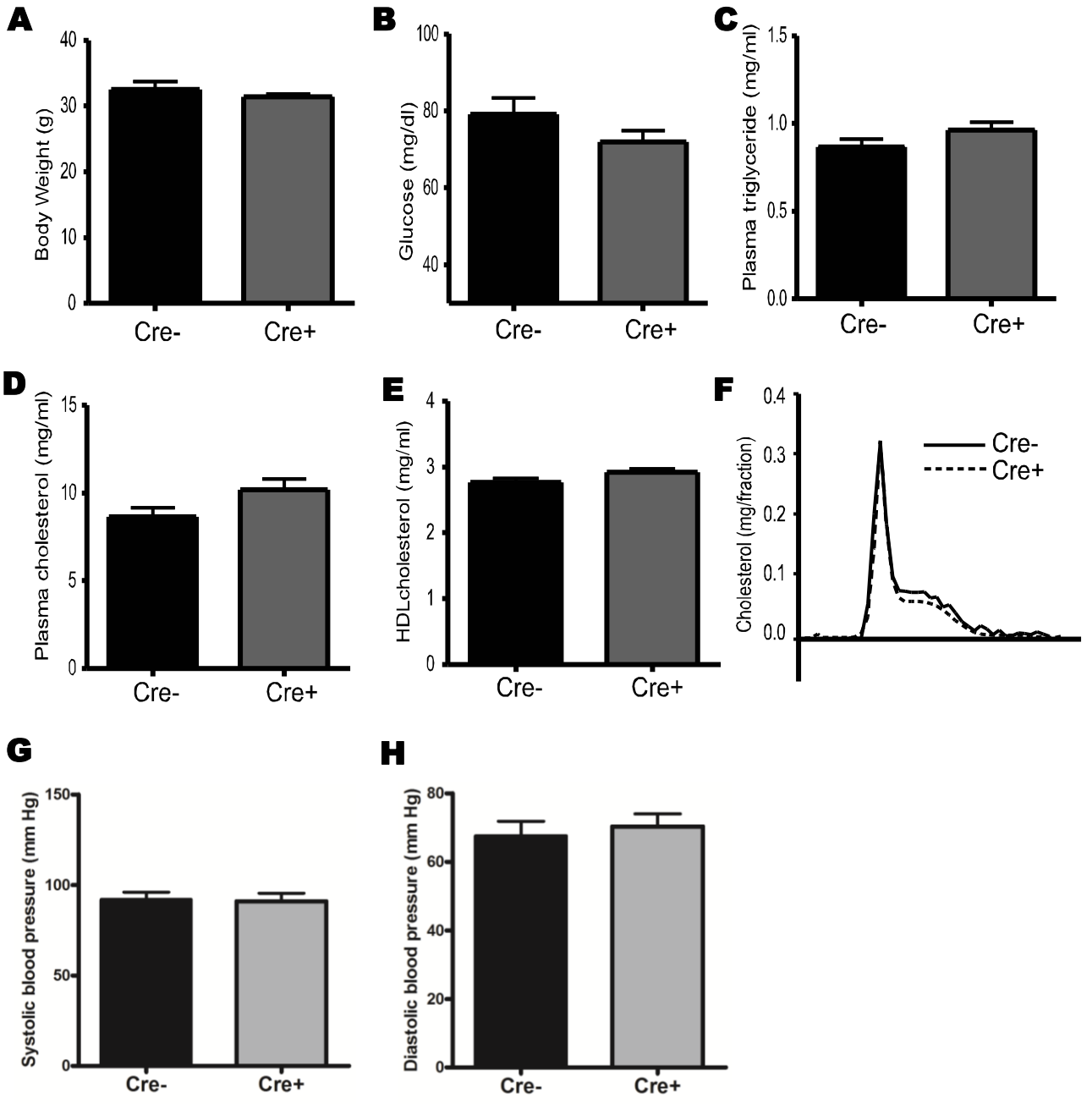
Chop^{fl/fl}Apoe^{-/-} and 11 *Chop^{fl/fl}SM22 α -CreKl⁺Apoe^{-/-}* lesions. *Arrow*, KLF4/ATF4/DAPI triple-stained nuclei. **B**, Representative Z series projection images of ATF4 (red), and α -actin (green), and DAPI (blue) staining in *Chop^{fl/fl}SM22 α -CreKl⁺Apoe^{-/-}* lesions and percentage of ATF4/ α -actin/DAPI triple-stained cells in 10 *Chop^{fl/fl}Apoe^{-/-}* and 8 *Chop^{fl/fl}SM22 α -CreKl⁺Apoe^{-/-}* lesions. *Arrow*, ATF4/ α -actin/DAPI triple-stained cells. Scale bar, 100 μ m.

Online Figure VIII. Proteasome-mediated degradation of HIF1 α and NFR2 is similar in control and CHOP-deficient VSMCs. *Chop^{fl/fl}Apoe^{-/-}* and *Chop^{fl/fl}SM22 α -CreKl⁺Apoe^{-/-}* VSMCs were pre-treated with 2.5 μ g/ml tunicamycin (Tm) for 16 h and then incubated for 1-8 h with either 10 μ g/ml cycloheximide (CHX) (**A, B**) or MG132 (**C, D**). Cell extracts were then immunoblotted for HIF1 α (**A, C**) and NFR2 (**B, D**). β -actin was included as loading control.

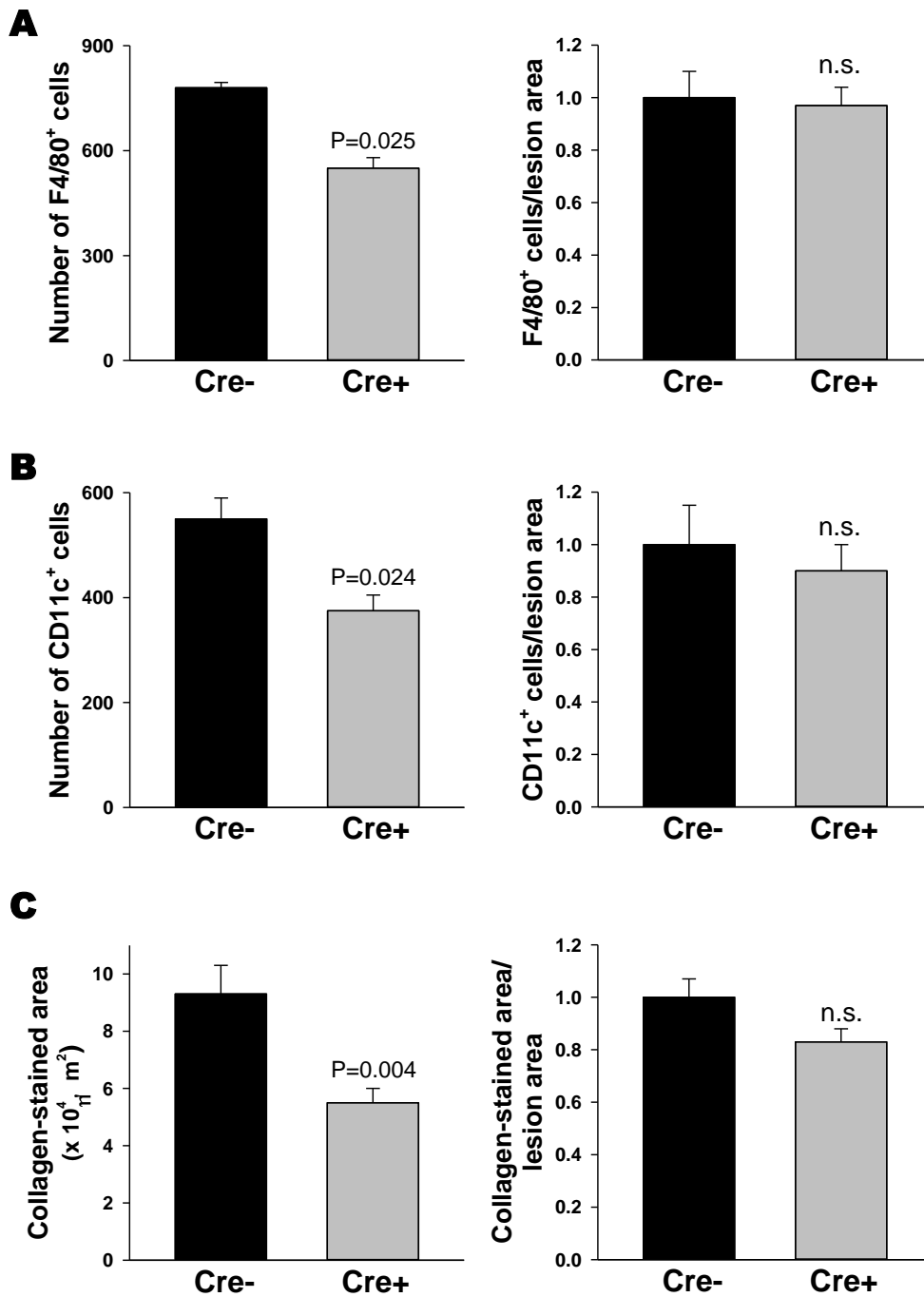




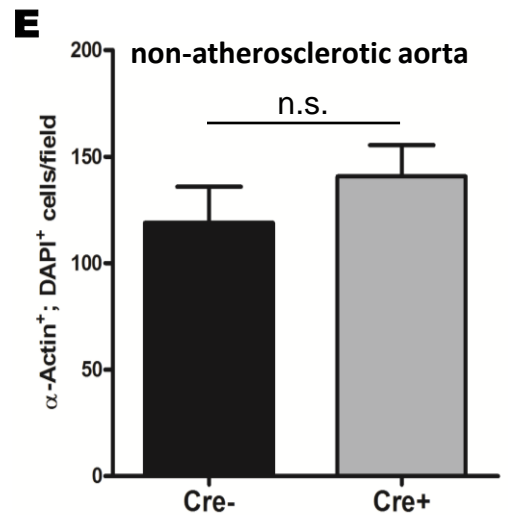
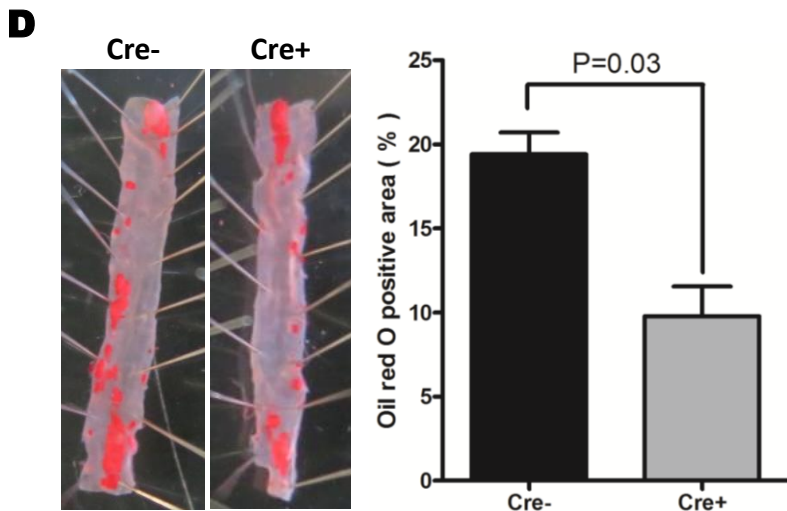
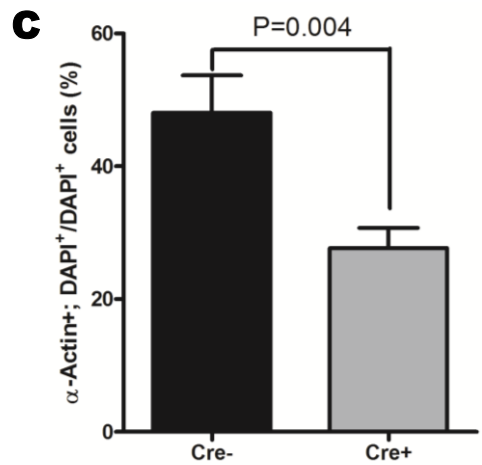
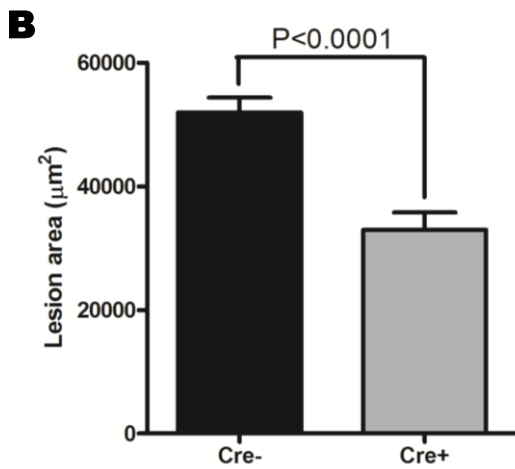
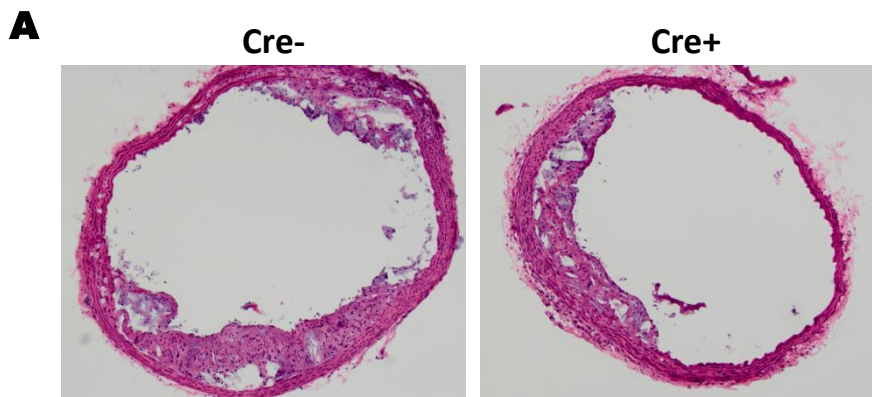
Online Figure II



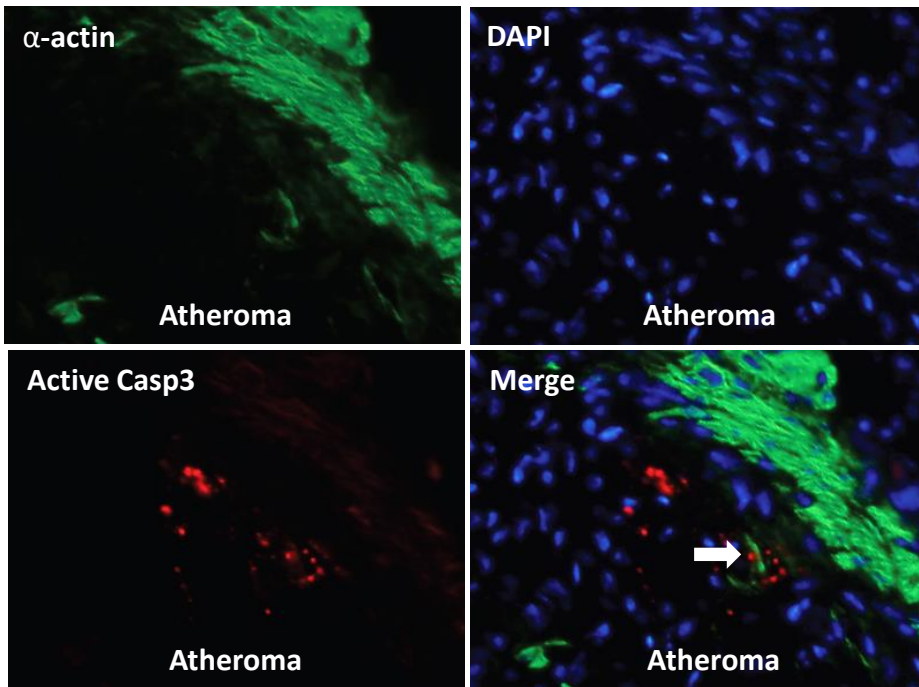
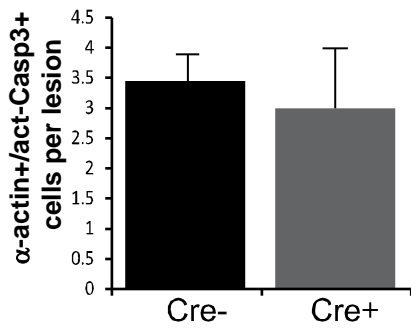
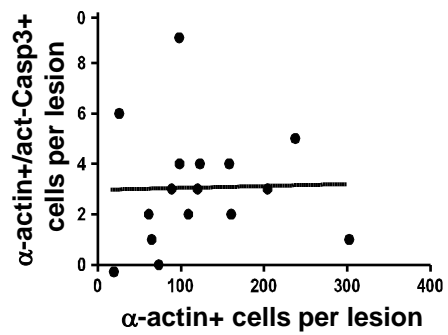
Online Figure III



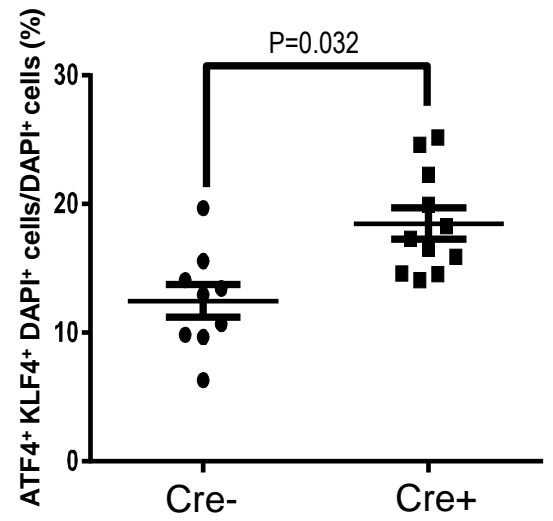
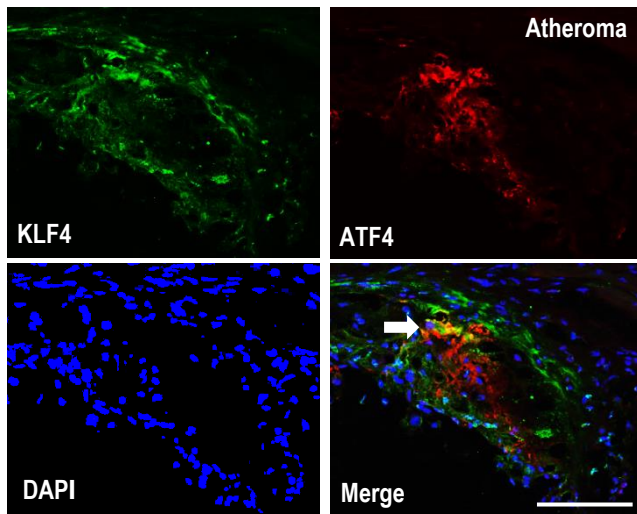
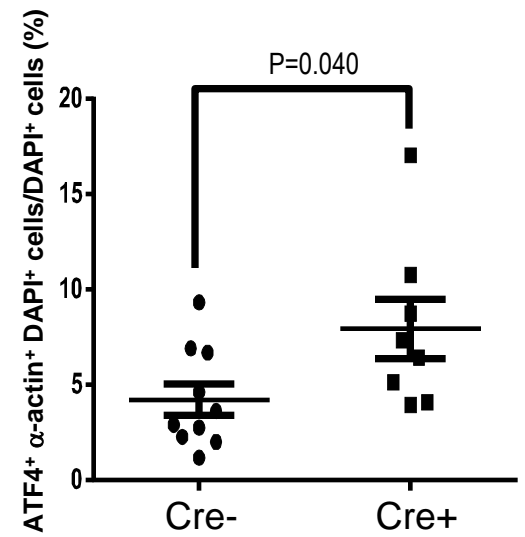
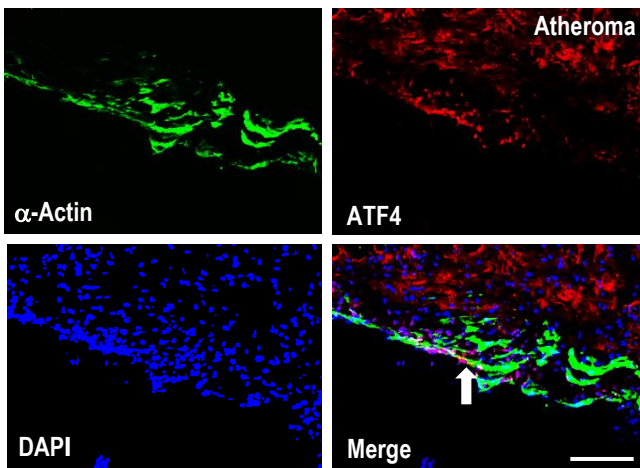
Online Figure IV

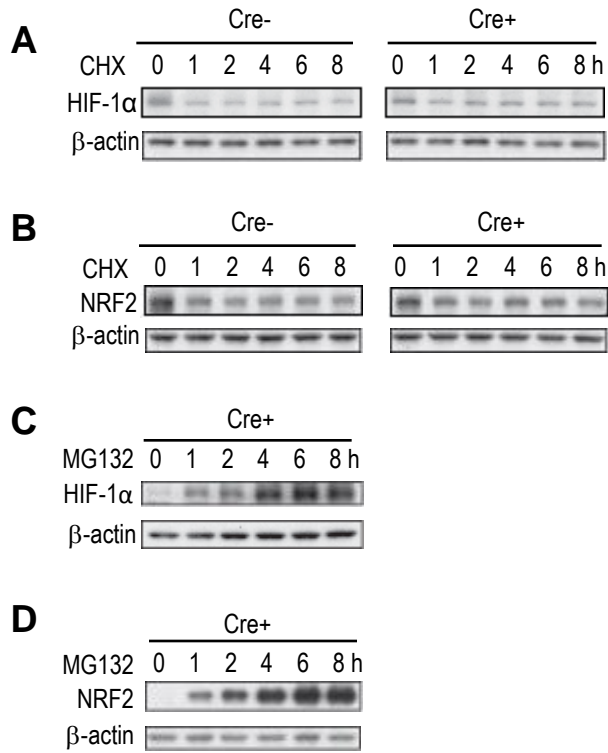


Online Figure V

A**B****C**

Online Figure VI

A**B**



Online Figure VIII